Elastic properties and phase diagram of the rare-earth monopnictide TbSb

Yoshiki Nakanishi,* Takuo Sakon,† and Mitsuhiro Motokawa
Institute for Materials Research, Tohoku University, Sendai 980-8577, Japan

Michiaki Ozawa and Takashi Suzuki
Graduate School of Science, Tohoku University, Sendai 980-8578, Japan

Masahito Yoshizawa
Department of Materials Science and Engineering, Iwate University, Morioka 020-8551, Japan
(Received 15 April 2003; revised manuscript received 19 May 2003; published 21 October 2003)

We have investigated the magnetic and elastic properties of rare-earth monopnictide TbSb by means of specific heat, high-field magnetization, and ultrasonic measurements. A pronounced anomaly was observed in the specific heat and elastic constants at an antiferromagnetic transition of $T_N = 15.5$ K. A pronounced softening towards low temperatures in $(C_{11}-C_{12})/2$ and C_{44} suggests that a degree of orbital freedom plays an important role at low temperatures. Furthermore, the high-field magnetization measurement exhibits an unexpected metamagnetic transition: clear three sharp steps. This was observed only for $H//\langle 111\rangle$, while only one step was observed for $H//\langle 100\rangle$ and $\langle 110\rangle$. The established (H-T) phase diagram from the present experimental results consists of mainly four phases. The obtained (H-T) phase diagram is discussed in terms of magnetic and quadrupolar interactions.

DOI: 10.1103/PhysRevB.68.144427 PACS number(s): 75.20.Hr, 71.27.+a, 71.70.Ch, 75.30.Mb

I. INTRODUCTION

The technical progress of both experimental measurements and purity of grown samples can advance the investigation of solid state physics. They occasionally help us find new phenomena in materials which had been studied for a long time. The rare-earth monopnictides, which are described as R-X_p (R=rare earth, X_p=N, P, As, and Sb) are classified into such materials. They exhibit a wide variety of attractive phenomena as changing R or X_p, such as magnetic ordering, heavy fermion system, intermediate valence state, and so on, although they crystallize in simple rocksalt type.[1,2] Thus, they have been studied for almost three decades. However, the difficulty of growing the single crystalline prevented the progress of the investigation. Recently, Suzuki *et al.* succeeded in growing high quality single crystalline samples and the study of rare-earth monopnictides began again.

The Tb monopnictide TbX_p has not been studied very intensively and deeply using the single crystalline sample so far because of the difficulty of the crystal growth. Recently, the de Haas–van Alphen (dHvA) signals were observed and the Fermi surface was investigated in detail by using the present crystal by our group. This experimental fact ensures that the samples is of high quality. The details are described in a separate article.[3] The lattice constant is well fitted by the rare-earth contraction as Tb^{+3}. Furthermore, TbSb is expected to be a well-localized $4f$-electron system according to our dHvA measurement. Therefore, it is considered that the Tb ion in TbX_p is trivalent with a $4f^8$ configuration. The neutron inelastic scattering measurements indicate that the ground state with the spin-orbit split $J=6$ splits into Γ_1 (singlet), Γ_2 (singlet), Γ_3 (doublet), Γ_4 (triplet), $\Gamma_5^{(1)}$ (triplet), and $\Gamma_5^{(2)}$ (triplet) with the Γ_1 (singlet) as the ground state.[4] The interesting feature of this material is that the nonmagnetic Γ_1 (singlet) ground state of the Tb ion is separated by a small energy gap from the first excited state Γ_4 (triplet).[4–6] This gives rise to an induced-moment ordering, which is dealing with the so called ''singlet-ground-state problem.'' On the other hand, PrSb and TmSb do not exhibit magnetic ordering although the Γ_1 singlet ground state is realized.[2] The reason for this difference is considered to be due to the energy competition between magnetic interactions and the difference of energy between the ground state and first excited one. That is to say, if the magnetic interaction in the first magnetic excited state is larger than the energy between the Γ_1 singlet ground state and the first excited one they exhibit a magnetic ordering. The difference of energy between them is estimated as PrSb for 73 K,[7] TmSb for 25 K,[8] and TbSb for 12 K.[5] All of the TbX_p compounds actually exhibit magnetic ordering. TbSb shows antiferromagnetic (AF) ordering of type II (MnO-type) with the $\langle 111\rangle$ easy axis at $T_N = 14.2$ K.[9] The ordered magnetic moment is estimated to be $8.2\mu_B$. This value is almost same as the value of $9\mu_B$ expected from the gJ. Furthermore, the structural phase transition from cubic to trigonal occurs at $T_N = 14.2$ K indicating that the orbital angular momentum strongly coupled with the spins through the spin-orbit coupling.[10] Thus, it seems that the quadrupolar moment also plays an important role in addition to the magnetic moment in this system. Due to the coexistence of spin and orbital degrees of freedom, the complicated magnetic structure is expected in magnetic fields. However, detailed low-temperature properties of TbX_p have not been clarified yet by using the high quality single crystals, although some studies had been done about three decades ago.[4–11] In this paper, we report on the detailed low-temperature physical properties of TbSb by means of specific heat, magnetization, and ultrasonic measurements, and discussed the physical interpretation of the newly established (H-T) phase diagram. Our results indicate that a phase in-

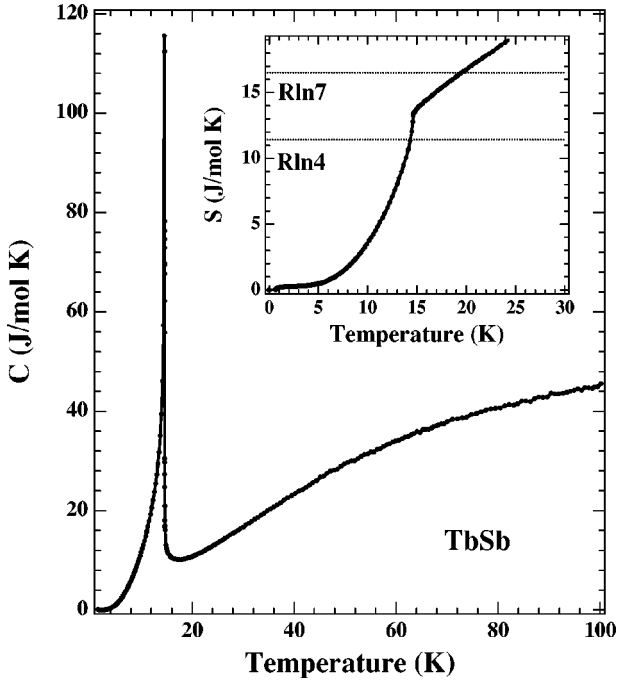

FIG. 1. Temperature dependence of the specific heat of TbSb. The inset shows the temperature dependence of the magnetic entropy.

duced by the magnetic fields appears and that the obtained results can be explained well by the previously proposed CEF level scheme for Tb^{+3} in TbSb taking into account both the magnetic and quadrupolar interactions. The preliminary studies have been published in Ref. 12.

II. EXPERIMENTAL

The single crystalline TbSb sample was prepared by Bridgeman method in a closed tungsten crucible. The magnetization (M) measurements were performed with a standard pick-up coil system up to 30 T by using the pulsed magnetic field and at temperatures down to 0.5 K using a ^{3}He cryostat. The specific heat (C) measurement was performed with a quasiadiabatic heat pulse method in magnetic fields along the $\langle 001 \rangle$ direction. The phonon contribution is subtracted by using the specific heat of LaSb. The elastic constants (c_{ij}) were measured by an ultrasonic apparatus based on a phase comparison method. The plates of quartz and $LiNbO_3$ were used for the piezoelectric transducers. The fundamental resonance frequency of quartz and $LiNbO_3$ transducers is 10–30 MHz. The transducers were glued on the parallel planes of the sample by an elastic polymer Thiokol.

III. EXPERIMENTAL RESULTS

A. Specific heats measurement

We first show the temperature dependence of the specific heat $C(T)$ in zero field in Fig. 1. In zero field, a prominent sharp peak is observed at 15.5 K. This peak was already reported and found it due to antiferromagnetic ordering.

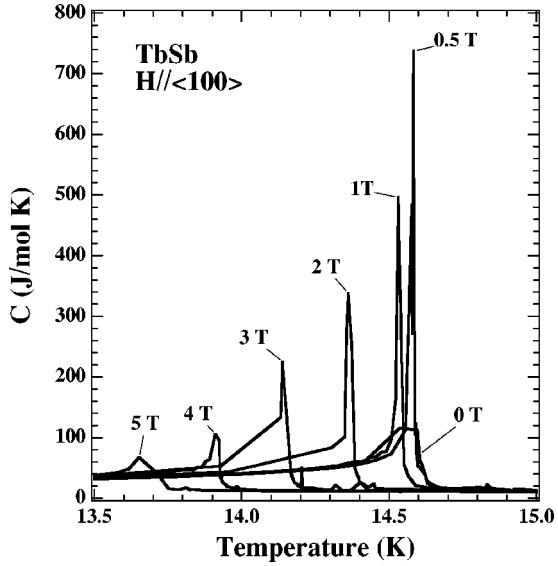

FIG. 2. Temperature dependence of the specific heat of TbSb under magnetic fields along the $\langle 100 \rangle$ axis.

However, the peak is sharp considerably and the peak value is four times larger than that in the previous result, and T_N is higher than the previous one 14.2 K,[6] indicating a good quality of our single crystal sample. The inset of Fig. 1 shows the estimated entropy S by integrating C/T curve with respect to T. At T_N, S reaches $R \ln 4 = 11.5$ J/mol K, which is close to the expected value of Γ_1 singlet ground state and Γ_4 triplet state. This result suggests that the magnetic ordering below T_N is ascribed to the Γ_4 triplet state. Figure 2 shows $C(T)$ under several fixed fields up to 5 T. With increasing magnetic field, the anomaly shifts to lower temperature and becomes smaller and broader.

B. Magnetization measurement

Next, we show the results of magnetization measurement on TbSb. Figure 3 shows the magnetization (M-H) curves

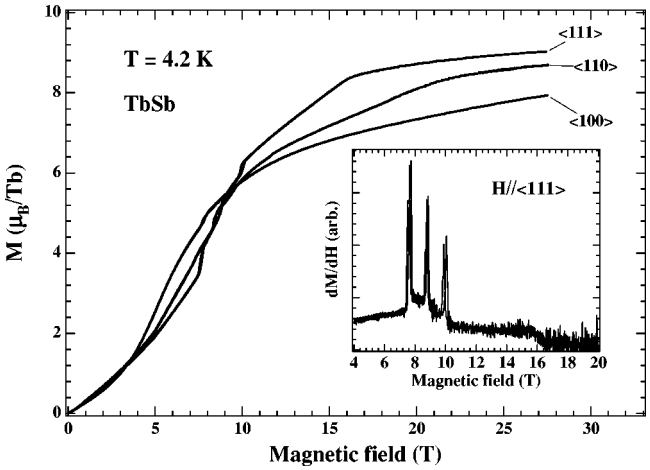

FIG. 3. Magnetization of TbSb for the principal axes in TbSb. The inset shows the differential magnetization dM/dH for $H//\langle 111 \rangle$.

for the field along principal axes $H//\langle 100\rangle$, $\langle 110\rangle$, and $\langle 111\rangle$ at 4.2 K. In the low-field region below 4 T, M-H curve shows such a small magnetic anisotropy. A sharp metamagnetic transition H_c is observed below T_N for $H//\langle 100\rangle$, $\langle 110\rangle$. This result is in good agreement with the previous result.[11] However, the present metamagnetic transition is quite sharper than previous one, indicating that present single crystal sample is of high quality and the magnetization measurement by using pulsed magnetic field is superior to observe the transition than that by using static magnetic field. It is noteworthy that a sharp three-step metamagnetic transition is found only for $H//\langle 111\rangle$ at 8, 9, 10 T in turn, although only one-step transition was observed in the previous measurement.[11] The inset of Fig. 3 shows the differential magnetization dM/dH for $H//\langle 111\rangle$. All metamagnetic transition are accompanied by a slight hysteresis indicating the first order nature. In the low-field region, a slight convex M-H curvature is observed, while in the high-field region a slight concave one is observed for three principal axes. A clear three anomaly was observed and guaranteed the intrinsic three-step structure in the magnetization curves for $H//\langle 111\rangle$. The magnetization almost saturated in high magnetic fields of 30 T with a value of $9.0\mu_B$/Tb, which is very close to the Tb^{+3} free-ion value of $gJ=9.0\mu_B$/Tb. Furthermore, the observed anisotropy of magnetization in high magnetic fields is in order of $M^{\langle 111\rangle}>M^{\langle 011\rangle}>M^{\langle 001\rangle}$ reflecting the ground state split by CEF effect, that is, Γ_1-Γ_4 states.

C. Ultrasonic measurement

Figure 4 shows the temperature dependence of elastic constants. The C_{11}, $C_L=(C_{11}+C_{12}+2C_{44})/2$ with longitudinal modes and C_{44}, $(C_{11}$-$C_{12})/2$ with transverse modes slightly increase with decreasing the temperature and exhibit a softening towards low temperature. Below T_N a hardening is observed in all of elastic constants. The dotted line in Fig. 4 is the theoretical result based on the following formula:[13–15]

$$C_\Gamma(T)=C_\Gamma^{(0)}(T)-\frac{Ng_\Gamma^2\chi_\Gamma^{(s)}(T)}{1-g_\Gamma'\chi_\Gamma^{(s)}(T)}, \tag{1}$$

where g_Γ' is the interionic quadrupolar coupling constant and N is the number of ions in a unit volume. $\chi_\Gamma^{(s)}$ is the single ion quadrupolar strain susceptibility, which is described in a cubic CEF potential as

$$\chi_\Gamma^{(s)}(T)=\sum_{ik}\frac{\exp(-E_{ik}^{(0)}/k_BT)}{Z}\times\left(\frac{1}{k_BT}|\langle ik|O_\Gamma|ik\rangle|^2-2\sum_{jl}\frac{|\langle ik|O_\Gamma|jl\rangle|^2}{E_i-E_j}\right), \tag{2}$$

where $|ik\rangle$ represents the kth eigenfunction of the ith CEF level. C_L^0 is the background part of elastic constants. In the present case of TbSb, the Curie term in the single ion quadrupolar strain susceptibility due to the Γ_4 triplet first excited state with orbital degeneracy gives rise to the elastic softening proportional to reciprocal temperature at low temperatures. The proposed level scheme by other experiments was adopted here, which will be discussed later in detail. Figure 5 shows the temperature dependence of C_L under several fixed fields along $\langle 110\rangle$ axis up to 6 T. The behavior of C_L around T_N is a little bit different from that of others. That is to say, two distinct anomalies were observed. With increasing magnetic field, the anomaly shifts to lower temperature. The absolute values of each elastic constant and calculated bulk modulus $C_B=(C_{11}+2C_{12})/3$ and Poisson ratio $\gamma=C_{12}/(C_{11}+C_{12})$ from C_{11} and $(C_{11}-C_{12})/2$ at both 77 and 4.2 K are listed in Table I.

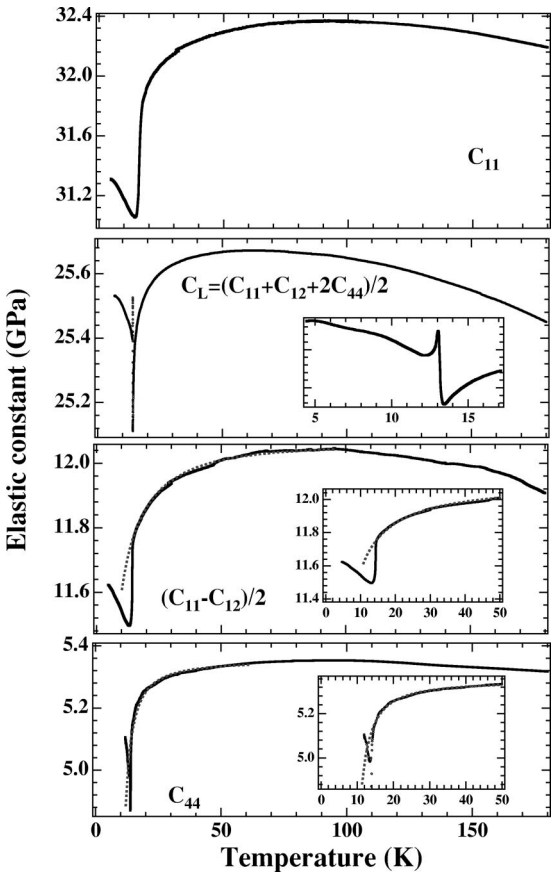

FIG. 4. Temperature dependence of the elastic constants C_{11}, $C_L=(C_{11}+C_{12}+2C_{44})/2$, $(C_{11}-C_{12})/2$ and C_{44} in TbSb. The black dots are the experimental data. The gray dots in the $(C_{11}-C_{12})/2$ and C_{44} indicates the calculated curves with Eq. (1). The insets show the low temperature part of the elastic constants of TbSb.

D. Magnetic phase diagram of TbSb

Figure 6 shows the magnetic field-temperature (H-T) phase diagram of TbSb for $H//\langle 100\rangle$ and $H//\langle 111\rangle$ determined by the present results of the specific heat, magnetization, and elastic constants. One can find that there are mainly two phases as indicated by Roman numerals letters I and II. As reported previously, the phase I and II are paramagnetic phase and AF magnetic one with type II magnetic structure, respectively.[9] Figure 6 also shows the (H-T) phase diagram

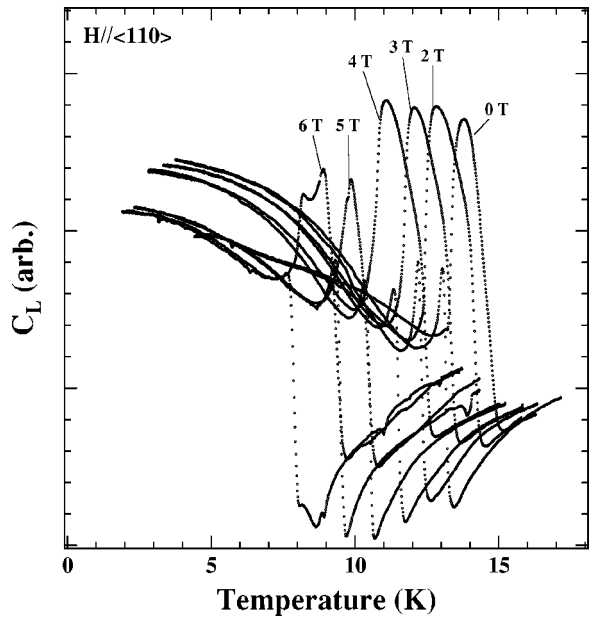

FIG. 5. Temperature dependence of the elastic constant C_L in TbSb under the selected magnetic field along the $\langle 110 \rangle$ axis.

of TbSb for $H//\langle 111 \rangle$ determined by the magnetization measurement. To the contrary, one can find additional phases as indicated by II-1 and II-2. This is the first finding by present studies. The both intermediate metamagnetic phases II-1 and II-2 are reduced with increasing temperature and disappear at about 14 K. The magnitude of magnetization for $H//\langle 111 \rangle$ is estimated to be of $4\mu_B$/Tb, $5\mu_B$/Tb, and $6\mu_B$/Tb for the phases II, II-1, and II-2, respectively. A slight hysteresis seems to appear at the three transition temperatures.

IV. DISCUSSIONS

We would like to examine the level scheme of Tb^{3+} ion split by the crystalline electric field (CEF) effect. Based on the obtained specific measurement and corresponding entropy, the ground state and first excited one are most likely to be Γ_1 singlet and triplet states, respectively. The previous studies such as neutron scattering, specific heat, magnetic susceptibility indicated the level scheme as follows: $\Gamma_1(1)$-$\Gamma_4(3)$-$\Gamma_5^{(2)}(3)$-$\Gamma_2(1)$-$\Gamma_5^{(1)}(3)$-$\Gamma_3(2)$, where the number in parenthesis denotes a degree of degeneracy. An energy splitting Δ between the ground state Γ_1 (1) and the first excited one Γ_4 (3) was estimated as about 12 or 14 K. According to the point charge model calculated by Lea, Leask and Wolf and this proposed level scheme one can obtain the explicit level scheme of Tb^{3+} manifolds split by CEF effect as follows:[4,5,16] $\Gamma_1(0)$-Γ_4(14 K)-$\Gamma_5^{(2)}$(32 K)-Γ_2(67 K)-$\Gamma_5^{(1)}$(106 K)-Γ_3 (113 K). The present results support the previous level scheme proposed by other group. By employing this level scheme we obtained the calculated elastic constants with the parameters $g_{\Gamma 3}=10.1$ K, $g'_{\Gamma 3}=33$ mK for $(C_{11}$-$C_{12})/2$ and $g_{\Gamma 5}=3.13$ K, $g'_{\Gamma 5}=30$ mK for C_{44} (see Fig. 4). The positive values of $g'_{\Gamma 3}$ and $g'_{\Gamma 5}$ indicate the existence of ferroquadrupolar interactions in TbSb.

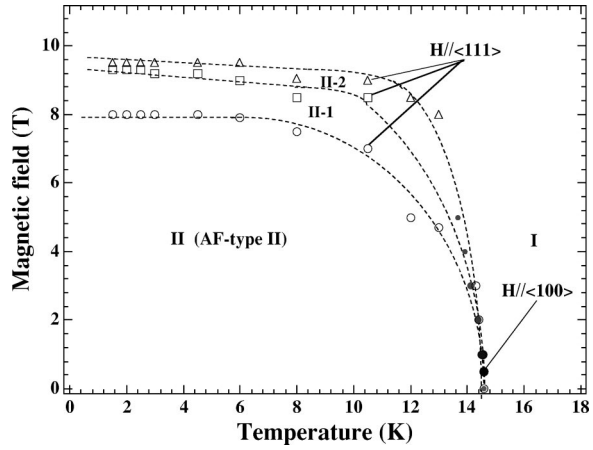

FIG. 6. (H-T) phase diagram in TbSb. The closed circle indicates the magnetic phase transition points for the field along $\langle 100 \rangle$ axis determined by the specific heat measurement. The opened symbols indicate the magnetic phase transition points for the field along $\langle 111 \rangle$ axis determined by the magnetization measurement. The dashed lines are guides to eyes.

TABLE I. The absolute values of each elastic constant and bulk modulus $C_B=(C_{11}+2C_{12})/3$ and Poisson ratio $\gamma=C_{12}/(C_{11}+C_{12})$ at both 77 and 4.2 K.

Mode	Elastic constants at 4.2 K	at 77 K
C_{11}	31.31 GPa	32.36 GPa
$C_L=(C_{11}+C_{12}+2C_{44})/2$	25.49 GPa	25.67 GPa
$(C_{11}-2C_{12})/2$	11.62 GPa	12.04 GPa
C_{44}	5.16 GPa	5.35 GPa
$C_B=(C_{11}+2C_{12})/3$	15.82 GPa	16.31 GPa
$\gamma=C_{12}/(C_{11}+C_{12})$	0.205	0.204

Next, we would like to discuss the obtained (H-T) phase diagram. The (H-T) phase diagram for $H//\langle 100 \rangle$ seems to be ordinal antiferromagnetic behavior. However, $H//\langle 111 \rangle$ is likely to be ascribed to a change of the magnetic structure in magnetic fields. As pointed out previously, the magnitude of induced magnetic moment in each phase gives us the significant information. The magnetization reaches $4.5\mu_B$/Tb at the first transition along $\langle 111 \rangle$ at 4.2 K. It reaches $5.0\mu_B$/Tb at the second transition and finally reaches $6.0\mu_B$/Tb at the third transition. The result of thermal striction gives a significant suggestion for the analysis. It indicated that the crystal structure changes from cubic to orthorhombic symmetry below $T_N=15.5$ K.[10] The magnetic moments are aligned ferromagnetically along the $\langle 111 \rangle$ axis in (111) layers and antiferromagnetically between the adjacent (111) layers below T_N.[9] As reported in other rare earth monopnictides such as DySb and HoP, the quadrupolar interactions cause the HoP-type ferromagnetic structure in which the magnetic moments couples perpendicularly due to the orbital restriction of $4f$ level.[17,18] Thus, in the intermediate metamagnetic phase for $H//\langle 111 \rangle$, it is natural to expect that the magnetic moments of some sites are directed to the $\langle 111 \rangle$ direction on considering the appearance of a large degree of magnetization.

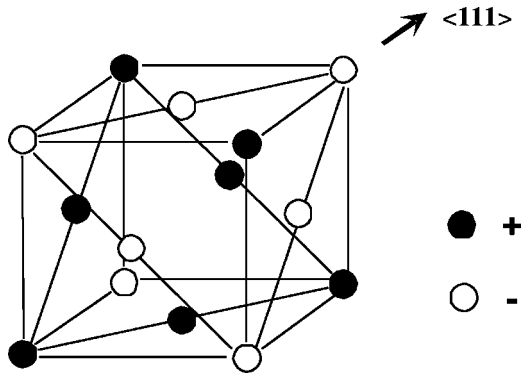

FIG. 7. The magnetic structure of TbSb (Type II antiferromagnet). The magnetic moments are aligned ferromagnetically in the (111) plane and antiferromagnetically in the adjacent layers, directed to the $\langle 111 \rangle$ axis.

Here, let us mention the possible magnetic structure of TbSb in magnetic fields. The magnetic unit cell has 14 magnetic ions for the present case TbSb as shown in Fig. 7. As mentioned above the magnetization along $\langle 111 \rangle$, e.g., the easy axis, is exactly 1/2 of the saturation value (M_0) at the first transition (H_1), which is compatible with the HoP-type spin structure. It reaches about 8/14 M_0 at the second transition (H_2), and about 10/14 M_0 or $1/\sqrt{2}M_0$ at the third transition (H_3). Taking account of only their magnetization values, the magnetic structures shown in Fig. 8 can be possible. Especially, the two magnetic structures can be proposed for phases II-1 and II-2. On the other hand, the magnetization is about $5\mu_B$/Tb for both $H//\langle 100 \rangle$ and $\langle 110 \rangle$. In the DySb case it shows the strong magnetic anisotropy, that is to say, the magnetization curves except for the easy axis are equal to the magnetization projected it on them, in agreement with the Ising model.[18] The metamagnetic transitions observed in DySb for principal axes also can be explained well by the Ising model. However, it is impossible to understand the magnetic anisotorpy and metamagnetic transitions of *M-H* curves of TbSb for principal on the analogy of DySb; the experimental facts such as one transition for $H//\langle 100 \rangle$ and $\langle 110 \rangle$, and three transitions for $H//\langle 111 \rangle$. It seems that they have their own magnetic structures for $H//\langle 100 \rangle$ and $\langle 110 \rangle$, independent of that for $H//\langle 111 \rangle$. The elastic neutron scattering measurement in magnetic field is strongly desired to determine the magnetic structure for principal axes.

Finally, we comment on the magnetic and quadrupolar interactions, quantitatively. The magnetic exchange interactions can be estimated by mean field theory. TbSb has an antiferromagnetic type-II magnetic structure in which Tb ion has a rigid $+3$ valence. The exchange interaction is described in terms of an interaction of each Tb^{3+} ion with its 12 nearest neighbors and with its 6 next-nearest neighbors. The experimental values of T_N and paramagnetic Curie temperature θ_p can be used to evaluate the exchange constants J_1 and J_2 with the mean field approximation. In this analysis it is assumed that exchange interactions other than those between nearest and next-nearest neighbors are negligible. The

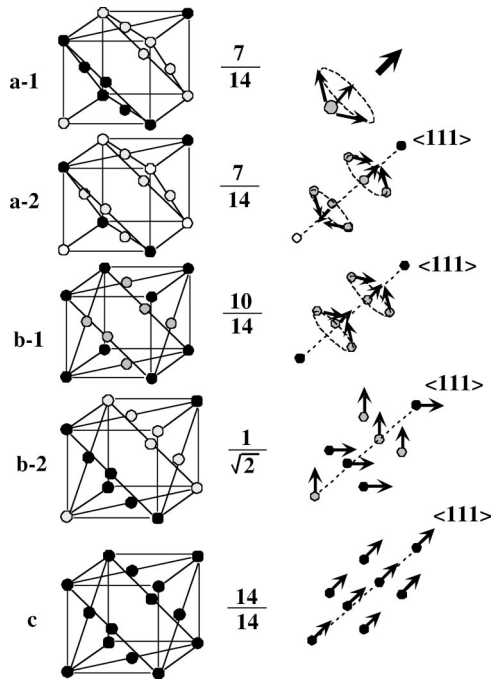

FIG. 8. The proposed magnetic structure of TbSb under fields for $H//\langle 111 \rangle$ in the phase II-1 (a1, 2), phase II 2 (b1, 2) and phase I (c). The closed and opened circles indicate the Tb ions whose moments are fully polarized ($9\mu_B$) and directed to the $\langle 111 \rangle$ axis and that in reverse, respectively. In (a1), the gray ones indicate those whose moment is aligned perpendicular to the $\langle 111 \rangle$ axis and they coupled ferromagnetically one another in the (111) planes as expected in HoP-type structures. In (a2) and (b1), the gray circles mean Tb ions whose moments are pointing to different $\langle 111 \rangle$ axis as illustrated, which is so-called umbrella or cone structure. The three Tb ions produce the effective value of one full Tb ion's magnetic moment for the $\langle 111 \rangle$ direction. In (b2), the canted antiferromagnetic structure is realized, in which magnetic moment (111) plane angles are 45° as shown in the figures. These magnetic structures lead to the same magnetization value as that observed in the present measurement.

equations relating T_N and θ_p for a type-II ordering antiferromagnet with $J=6$ are

$$k_B T_N = -168 J_2, \tag{3}$$

$$k_B \theta_p = 336 J_1 + 168 J_2. \tag{4}$$

Using the values of $T_N = 15.5$ K and $\theta_p = -14$ K,[3] the values of J_1 and J_2 are found to be 0.003 and -0.04 K, respectively for TbSb. Thus the exchange field is estimated by means of J_1 and J_2 in TbSb,

$$H_{\text{exchange}} = \lambda M = \sum_{\text{i}} \frac{z_i}{g^2 \mu_B N} J_i M = 34.4T, \tag{5}$$

where g is Lande's g factor, N is the number of atoms in unit volume, z_i is the number of the ith neighbor's atom ($i = 1, 2$). M is used as $8.2\mu_B$ which is the value of magnetic moment in the ordered state determined by the neutron diffraction measurement.[9] Roughly speaking, this value is close

to that at which the magnetization curve saturates for $H//\langle 111\rangle$. On the other hand, the quadrupolar interaction was estimated to be 33 mK for Γ_3 and 30 mK for Γ_5, respectively. These estimated values remind us that the important interactions and CEF splitting energy: energy separation between the singlet ground state and first excited state are in competition one another. The present results of ultrasonic measurement indicates that the AF magnetic exchange and the electric ferroquadrupolar interactions are active among Tb^{3+} in TbSb. The quadrupolar interaction among quadrupolar moments is probably not so strong to induce the structural phase transition in TbSb. However, the quadrupolar ordering can be stabilized in the magnetic fields, as seen in other rare-earth compounds such as CeB_6 and TmTe.[19–24] The obtained results let us conjecture that the magnetic phase transition causes the quadrupolar ordering. In fact, a shape of the transition at 15.5 K in the specific heat becomes sharper by applying the tiny magnetic fields, indicating the stabilization of the ordered phase. Furthermore, the first-order-like transition on the boundary between phases I and II suggests that the AF magnetic ordering and the ferroquadrupolar ordering may occur simultaneously.[25–27] In particular, the latter one causes the pronounced structural phase transition from cubic to orthorhombic symmetry below 15.5 K, as seen in thermal striction measurement. This situation is probably similar to that of TbP reported by Bucher *et al.*[28]

V. CONCLUDING REMARKS

In this paper, we have presented the elastic and magnetic properties of rare earth-monopnictide TbSb. From our experiments we obtain the following conclusions. The elastic softening towards low temperatures was observed in all measured elastic constants. They are ascribed mainly to the first excited state Γ_4 (triplet), which locates close to the singlet ground state Γ_1. We found that the high-field magnetization measurement exhibited an unexpected metamagnetic transition: the clear three sharp steps only for $H//\langle 111\rangle$ and established a new (H-T) phase diagram. We estimated the values of magnetic and quadrupolar interactions and proposed some possible magnetic structures in magnetic fields. Furthermore, we pointed out that the ferroquadrupolar interaction was active, and played a vital role at low temperatures. It is necessary to clear them by microscopic methods such as neutron scattering or x-ray resonant measurements in magnetic fields.

ACKNOWLEDGMENTS

The measurements have been performed in the Cryogenic Division of the Center for Instrumental Analysis, Iwate University. This work was supported by a Grant-in-Aid for Science Research from the Minister of Education, Culture, Sports, Science, and Technology of Japan.

*Electronic address: yoshiki@iwate-u.ac.jp. Present address: Department of Materials Science and Engineering, Iwate University, Morioka 020-8551, Japan. URL: http://espana.mat.iwate-u.ac.jp/yoshihp/

†Electronic address: sakon@ipc.akita-u.ac.jp. Present address: Department of Mechanical Engineering, Faculty of Engineering and Resource Science, Akita University, Akita 010-8502, Japan.

[1] T. Suzuki, Physica B **186-188**, 347 (1993).

[2] P. Wachter, *in Handbook on the Physics and Chemistry of Rare Earths*, edited by K.A. Gschneidner, Jr., L. Eyring, G.H. Lander, and G.R. Choppin (Elsevier, Amsterdam, 1994), Vol. 19, p. 388.

[3] Y. Nakanishi, M. Ozawa, T. Sakon, M. Motokawa, and T. Suzuki (unpublished).

[4] T.M. Holden, E.C. Svensson, W.J.L. Buyers, and O. Vogt, Phys. Rev. B **10**, 3864 (1974).

[5] Y.Y. Hsieh and M. Blume, Phys. Rev. B **6**, 2684 (1972).

[6] W. Stutius, Phys. Kondens. Mater. **9**, 341 (1969).

[7] K.C. Turberfield and L. Passel, J. Appl. Phys. **42**, 1746 (1971).

[8] O. Vogt and B.R. Cooper, J. Appl. Phys. **39**, 1202 (1968).

[9] H.R. Child, M.K. Wilkinson, J.W. Cable, W.C. Koehler, and E.O. Wollan, Phys. Rev. **131**, 922 (1963).

[10] F. Hulliger and F. Stucki, Z. Phys. B: Condens. Matter **31**, 391 (1978).

[11] A. Buschbeck, Ch. Chojnowski, J. Kötzler, R. Donder, and G. Thummes, J. Magn. Magn. Mater. **171-182**, 171 (1987).

[12] T. Sakon, Y. Nakanishi, M. Ozawa, T. Suzuki, H. Nojiri, and M. Motokawa, J. Magn. Magn. Mater. **177-181**, 3405 (1998).

[13] S. Nakamura, T. Goto, S. Kunii, K. Iwashita, and A. Tamaki, J. Phys. Soc. Jpn. **63**, 623 (1994).

[14] P.M. Levy, J. Phys. C **6**, 3545 (1973).

[15] V. Dohm and P. Fulde, Z. Phys. B: Condens. Matter **21**, 369 (1975).

[16] K.R. Lea, M.J.M. Leask, and W.P. Wolf, J. Phys. Chem. Solids **23**, 1381 (1962).

[17] G. Busch and O. Vogt, J. Appl. Phys. **39**, 1334 (1968).

[18] G. Busch, O. Marincek, A. Menth, and O. Vogt, Phys. Lett. **14**, 262 (1965).

[19] J.M. Effantin, J. Rossat-Mignod, P. Burlet, H. Bartholin, S. Kunii, and T. Kasuya, J. Magn. Magn. Mater. **47&48**, 145 (1985).

[20] O. Sakai, R. Shiina, H. Shiba, and P. Thalmeier, J. Phys. Soc. Jpn. **66**, 3005 (1997).

[21] P. Link, A. Gukasov, J.M. Mignot, T. Matsunura, and T. Suzuki, Phys. Rev. Lett. **80**, 4779 (1998).

[22] T. Matsunura, S. Nakamura, T. Goto, H. Amitsuka, T. Sakakibara, and T. Suzuki, J. Phys. Soc. Jpn. **67**, 612 (1998).

[23] Y. Kuramoto and N. Fukushiama, J. Phys. Soc. Jpn. **67**, 583 (1998).

[24] N. Fukushiama and Y. Kuramoto, J. Phys. Soc. Jpn. **67**, 2460 (1998).

[25] J. Sivardiere and M. Blume, Phys. Rev. B **5**, 1126 (1972).

[26] D.K. Ray and J. Sivardiere, Solid State Commun. **19**, 1053 (1976).

[27] S.J. Allen, Phys. Rev. **167**, 492 (1968).

[28] E. Bucher, J.P. Maita, G.W. Hull, Jr., L.D. Longinotti, B. Lüthi, and P.S. Wang, Z. Phys. B: Condens. Matter **25**, 41 (1976).